Finite-element simulations of split Hopkinson test of Ti-based alloy

M. Demiral[1, a], T. Leemet[2, b], M. Hokka[2, c], V. T. Kuokkala[2, d], A. Roy[1, e], V. V. Silberschmidt[1, f]

[1]Wolfson School of Mechanical and Manufacturing Engineering, Loughborough University, LE11 3TU, Leicestershire, UK.

[2]Department of Materials Science, Tampere University of Technology, Korkeakoulunkatu 6, 33720 Tampere, Finland.

[a]M.Demiral@lboro.ac.uk, [b]tonu.leemet@tut.fi , [c]mikko.hokka@tut.fi, [d]veli-tapani.kuokkala@tut.fi, [e]A.Roy3@lboro.ac.uk, [f]V.Silberschmidt@lboro.ac.uk

Keywords: Split Hopkinson Pressure Bar; Finite-element analysis; Ti-15-3-3-3.

Abstract. Ti-based alloys are extensively used in aerospace and other advanced engineering fields due to their high strength and toughness, light weight, excellent corrosion resistance and ability to withstand extreme temperatures. Since these alloys are hard to machine, there is an obvious demand to develop simulation tools in order to analyse the material's behaviour during machining and thus optimise the entire machining process. The deformation processes in machining of Ti-alloys are typically characterized by high strains and temperatures. Split Hopkinson Pressure Bar (SHPB) technique is a commonly used experimental method to characterize the material behaviour at high strain rates; the stress-strain relation of the material is derived from the obtained experimental data. A computational study on a three-dimensional finite element model of the SHPB experiment is performed to assess various features of the underlying mechanics of deformation processes at high-strain and -strain-rate regimes. In the numerical analysis, an inhomogeneous deformation behaviour is observed in the workpiece at the initial stages of compression contrary to a standard assumption of stress and strain homogeneity in the specimen.

Introduction

Titanium alloy Ti-15V-3Cr-3Al-3Sn, commercially known as Ti-15-3-3-3, is a metastable beta alloy. Beta-titanium alloys show a unique combination of high strength, high ductility, low density and corrosion resistance. These properties make these alloys ideal for aerospace engineering applications, power generation, and the chemical industry [1]. Since these alloys are hard to machine, there is an obvious demand to develop simulations tools in order to analyse the material's behaviour during machining and thus optimise the entire machining process. Typically, the deformation processes in machining are characterized by high strains and temperatures. Therefore, obtaining the material properties at these extreme conditions is essential for accurate computational modelling purposes. There are several experimental methods for measuring the material response under high strain rates including, for example, drop tower tests and cam plastometers [2]. However, the most commonly used testing method at strain rates between 10^2 and 10^4 s^{-1} under varying temperature regimes is the Split Hopkinson Pressure Bar (SHPB) technique [3].

The assessment of stress-strain relationship based on SHPB experimental analysis employs some basic assumptions: First, the wave propagation in the bars is assumed to be adequately described with the one-dimensional elastic wave propagation theory. Secondly, the stress and strain fields in the specimen are assumed to be homogeneous in the axial direction, and finally, the radial inertial effects of the specimen as well as friction effects are considered to be negligible. An excellent review of the consequence of these assumptions on the accuracy and relevance of SHPB is summarized in [4]. Numerical and experimental studies carried out in [5, 6, 7, 8, 9] demonstrated that stresses and strains are not axially uniform, especially in the early stage of the experiment. Thus, there is a need to critically reassess the validity of the assumptions in the determination of the mechanical response of recently introduced advanced alloys such as Ti-15-3-3-3. In this study, a three-

dimensional finite element (FE) simulation of the SHPB test is carried out to better understand the spatio-temporal realization of deformation mechanism in specimen during the impact.

Split Hopkinson Bar Technique

The construction of a compression SHPB system is illustrated schematically in Fig. 1. The system consists of two 1.2 m-long maraging steel rods with a diameter of 21.77 mm (incident and transmitter bar) and a striker bar made of the same material and with the same diameter [10]. The striker bar is shot against the free end of the incident stress bar, which on impact generates a stress pulse that propagates in the incident bar towards the specimen that is sandwiched between the incident and transmitter bars [3].

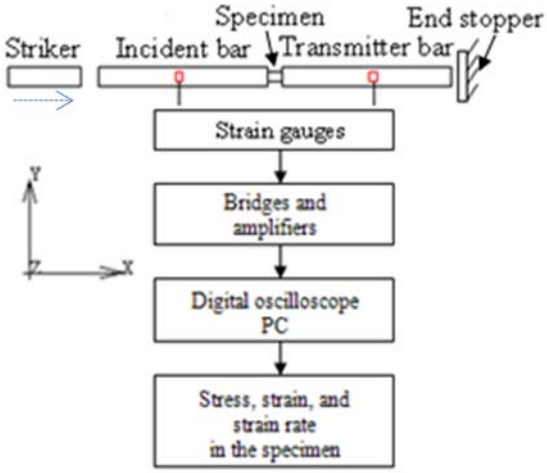

Figure 1: Schematic of SHPB technique [11].

As the stress pulse reaches the bar-specimen interface, part of the pulse is reflected back as an elastic wave while the remainder is transmitted through the specimen to the transmitter bar. The specimen is deformed plastically at a high strain rate as the pulse travels through it. Typically, several reverberations within the specimen are required to build up an equilibrium stress. Axial components of the stress (σ), strain (ε), and strain rate ($\dot{\varepsilon}$) in the specimen can be calculated from the three time-dependent elastic stress pulses, namely, incident (ε_I), reflected (ε_R) and transmitted (ε_T) pulses, measured from the pressure bars using strain gauges and recorded with a digital oscilloscope. In the case of dynamic equilibrium, i.e., the stress is uniform across the specimen, equations for strain rate, strain and stress can be expressed as follows:

$$\dot{\varepsilon}(t) = -\frac{2C}{L_S}\varepsilon_R(t), \tag{1}$$

$$\varepsilon(t) = -\frac{2C}{L_S}\int_0^t \varepsilon_R\,(t), \tag{2}$$

$$\sigma(t) = \frac{A_B E_B}{A_S}\varepsilon_T(t)\ , \tag{3}$$

where C is the elastic wave velocity, L_S is the initial length of the specimen, A_B and A_S are the cross-sectional areas of the bars and the specimen, and E_B is the Young's modulus of the bar material. Eqs. 1 – 3 are known as the 1-D wave analysis of SHPB data [12].

The mechanical behaviour of Ti-15-3-3-3 under impact conditions is characterized with SHPB tests at strain rates ranging from 600 s^{-1} to 3500 s^{-1} at room temperature (20°C). For quasi-static conditions compression tests were performed on a servo-hydraulic testing machine. Specimens were wire-cut from an as-received ingot to cylinders of diameter 8 mm and length 6 mm. A length-to-diameter ratio of 0.5 to 1 is considered to be an optimum range to minimize the effects of specimen friction and inertia in SHPB [13]; the ratio for the specimen tested is 0.75. The properties and dimensions of the materials used in the experiments and, consequently, in finite element simulations are presented in Table 1. The strain-rate dependent stress-strain responses of Ti-alloy obtained from

the experiments are given in Fig. 2. It is observed that the flow stress increases noticeably with increasing order of magnitude in the strain rate at room temperature.

Table 1: Geometric parameters and material properties.

	Striker	Bars	Specimen
Material	Maraging steel	Maraging steel	Ti-15-3-3-3
Length [mm]	200	1200	6
Diameter [mm]	21.77	21.77	8
Young's modulus [GPa]	198	198	87
Poisson's Ratio	0.329	0.329	0.3
Density [kg/m^3]	8470	8470	4900

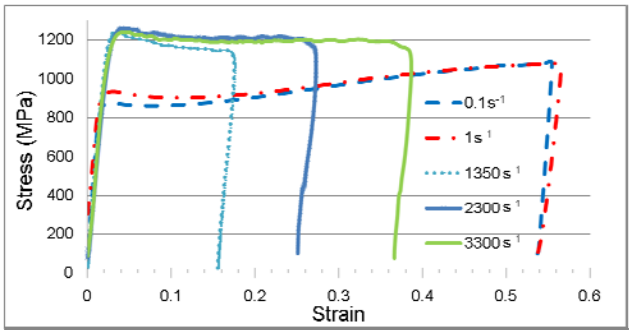

Figure 2: Stress-strain diagrams of Ti-15-3-3-3 obtained from SHPB tests (1350 s^{-1}, 2300 s^{-1}, 3300 s^{-1}) and quasi-static compression tests (0.1 s^{-1}, 1 s^{-1}) at room temperature (20°C).

Finite-Element Modelling

A numerical analysis was carried out to study the details of the underlying mechanics during the deformation process in the SHPB experiment. The commercial general purpose finite element code MSC.Marc [14] was used for a three-dimensional finite element model of the experiment (Fig. 3). The main components of the experiment setup, which are the striker bar, workpiece being tested, and the incident and transmitter bars were meshed with eight-noded, isoparametric, hexahedral elements (Element type 7). The incident and transmitter bars were discretized with 5760 elements each and the striker bar with 960 elements. The initial number of elements used to mesh the workpiece was 75600. An element-size-sensitivity analysis was carried out for the workpiece, and a 0.2 mm element size was found to be optimum for our numerical experiments. Automatic remeshing was used to update the mesh during the simulations in order to avoid high element distortion, which may lead to convergence errors. The displacement of right-hand side of transmitter bar is constrained in all directions to model the end stopper used in the experiments (Fig. 1). In the numerical analysis, the striker hits the incident bar with an initial velocity of 24.3 m/s, which roughly corresponds to a strain rate $(\dot{\varepsilon})$ of 2700 s^{-1}.

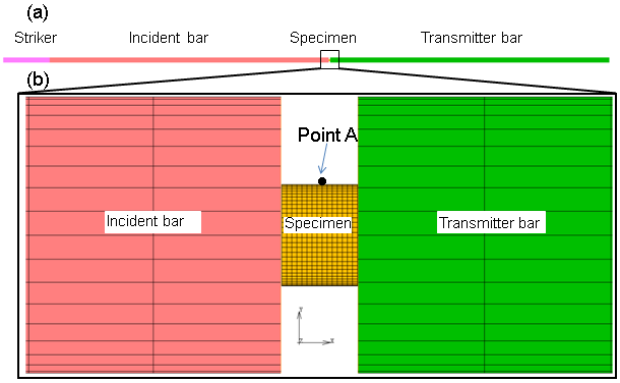

Figure 3: FE model of the SHPB experiment (a) and zoomed part with specimen tested (b).

Material model

A piece-wise linear elasto-plastic material model is used to represent the material behaviour in our numerical simulations. The model enables us to control the maximum stress values, for instance, the stress-strain curves obtained from the experiments (Fig. 2) were modified to limit the stress value magnitude by the respective ultimate tensile strength (UTS) values for high strains (Fig. 4).

Popular material models such as the Johnson-Cook model (and its variants) could also be used in our numerical simulations. However, this model predicts unrealistically high stress values for large strain and strain-rate values and hence avoided.

In order to account for higher strain rates beyond the experimentally characterized strain rates, the stress-strain data for a large strain rate value of 10^5 s^{-1} was chosen with a 20% offset from the corresponding values for 3300 s^{-1} (Fig. 4).

Experimental results characterizing the temperature-dependent thermal expansion coefficient and the specific heat value of the workpiece material (C_p) used in the simulations are published elsewhere [15].

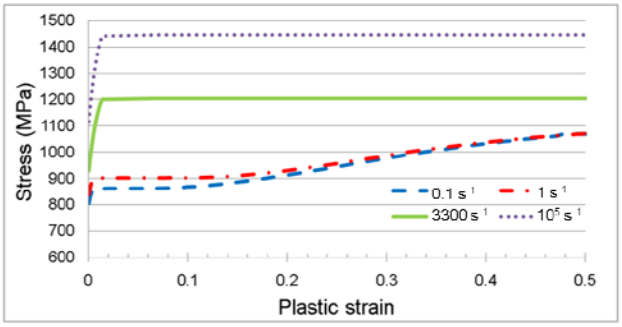

Figure 4: Modified strain rate-sensitive material model at room temperature (20°C).

Numerical results and discussion

The uniaxial stress-strain behaviour of the specimen was evaluated through the analysis of the incident, transmitted and reflected waves. The axial strain values at the middle span of the bars are determined in the numerical analysis and compared with the corresponding experimental results at the same physical locations where the strain gauges are attached (Fig. 1).

An axial impact of the striker bar on the incident bar results in the generation of a compressive pulse wave propagating in the incident bar. The initial response of the incident bar, i.e., the incident pulse, is obtained before compression of the specimen, while the dynamic plastic response of the workpiece is obtained via the transmitted and reflected pulses measured from the transmitter and incident bars, respectively. The FE numerical result characterising the axial strain waves matches reasonably well with the experimental data for the incident, transmitted and reflected waves (Fig. 5). The incident and transmitted pulses travelling through the bars have compressive characteristics;

on the other hand, the reflected pulse is primarily a tension wave. It may be assumed that various complicating factors such as (dynamic) friction between the workpiece and the pressure bars, longitudinal wave dispersion in the pressure bars, radial inertia in the workpiece, and impedance mismatch of the bars with the specimen is, possibly, responsible for the minor deviations of the simulation results from the experiments.

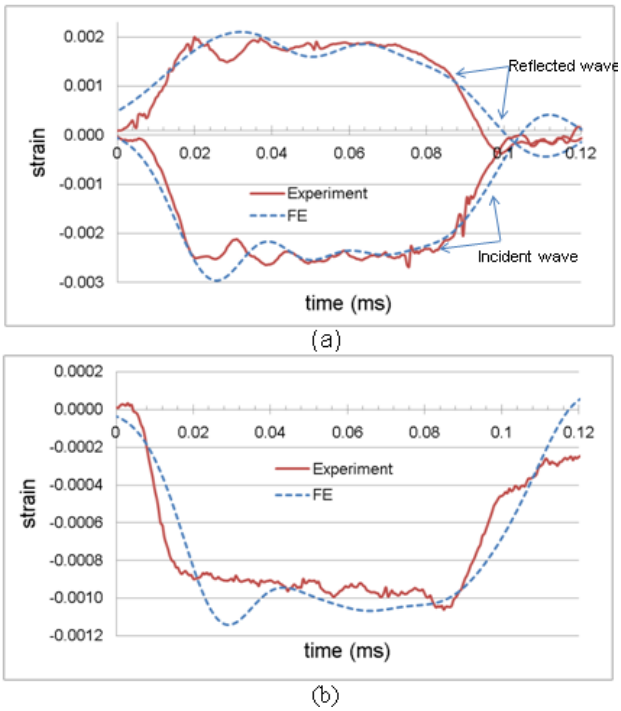

Figure 5: Comparison of strain evolution at the bar mid-span: (a) incident and reflected stress waves; (b) transmitted stress wave.

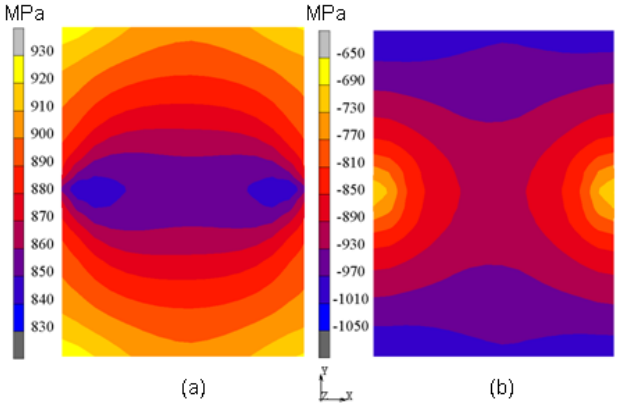

Figure 6: Distribution of von Mises (a) and axial stresses (b) in central cross sectional plane normal to the radial direction of specimen at t = 11.3 µs after first contact between incident bar and specimen.

The computational results also demonstrate that at the early stages of the compression process an inhomogeneous deformation behaviour is observed in the workpiece (Figs. 6 and 7) for both the elastic and plastic deformation regimes. A homogeneous stress state is reached in the workpiece at approximately 2% plastic strain. The magnitude of equivalent and axial stress value in the central cross sectional plane normal to the radial direction of the workpiece at t = 11.3 µs after first contact between incident bar and specimen vary by 100 MPa and 400 MPa , respectively (Fig. 6). The inhomogeneity is also observed in the equivalent plastic strain rate values at the same cross sectional plane of the workpiece (Fig. 7). These may be of some concern when deriving the relevant stress-

strain relations from the experimental procedure as one of the fundamental assumptions is that of a homogeneous stress state in the body during the entire deformation history.

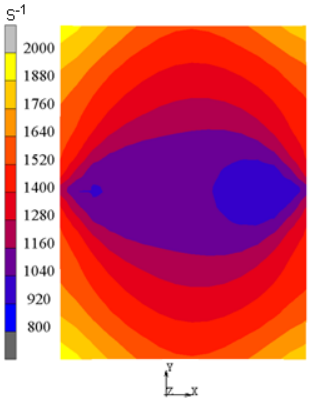

Figure 7: Equivalent plastic strain rate distribution in the central cross sectional plane normal to the radial direction of specimen at t = 12.5 μs after first contact between incident bar and specimen.

The workpiece material studied in this work, Ti-15-3-3-3, is a modest heat conductor (thermal conductivity is 8.08 W/m.K). The specimen, therefore, heats up considerably due to the plastic work done in the adiabatic deformation conditions of the studied case. Our numerical results demonstrate that the temperature in the workpiece increases noticeably during the test from 25°C to 93°C (Fig. 8). In the literature, the initial temperature of the specimen is commonly used as the reference temperature of the conducted experiment [16, 17]. However, adiabatic heating effects need to be accounted for and appropriately corrected while determining the isothermal mechanical stress-strain response. In other words, the constitutive models without accounting for adiabatic heating effects may lead to non-negligible errors while describing the plastic response of the materials under various loading conditions. It is especially important at elevated temperatures, where the temperature sensitivity of the material during the deformation process is larger. The same discussion can be extended to the reference strain-rate value, which is observed to be non-constant during the initial stages of the test (Fig. 7). Using a reference strain-rate value for the each experiment conducted without accounting for its variability during the compression may also lead to errors.

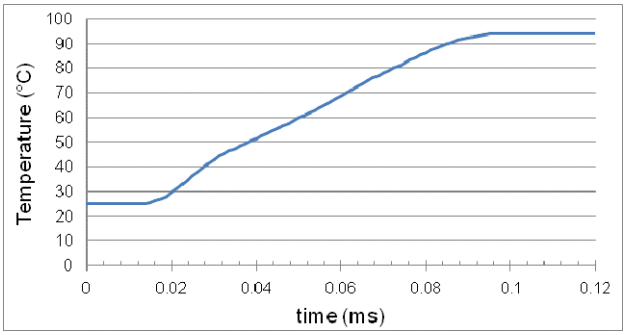

Figure 8: History of temperature distribution in the specimen during the compression process at point A (see Fig. 3).

Conclusion

In this study, a 3-D finite-element simulation of the split-Hopkinson pressure bar test was performed to study the deformation behaviour of a Ti-based alloy under high-strain and -strain-rate deformation regimes. The experiments were conducted at strain rates ranging from 600 s^{-1} to 3500 s^{-1} at room temperature to obtain the macroscale mechanical stress-strain response of the material to be consequently used to build an appropriate constitutive description of the material behaviour.

In the numerical analysis of the SHPB experiment at room temperature, an inhomogeneous deformation behaviour is observed in the workpiece at the initial stages of compression contrary to a

standard assumption of homogeneity of stress and strain fields in the specimen used to characterize the specimen's material behaviour. Thus, the validity of such assumptions should be critically assessed for each combination of material and high-strain-rate loading conditions.

In the SHPB approach, the obtained material data is referred to a constant (reference) temperature and strain rate. The adiabatic heating and variable strain rate during the compression process should, however, be taken into account in the experimental analysis and identification of the material model parameters, since this can result in non-adequate prediction of the real-life material properties. A modelling strategy addressing these mechanically relevant parameters is currently being developed and will be reported in the future.

Acknowledgement

Funding from the European Union Seventh Framework Programme (FP7/2007-2013) under grant agreement No. PITN-GA-2008-211536, project MaMiNa is gratefully acknowledged.

References

[1] C. Leyens and M. Peters (eds.): Titanium and Titanium Alloys – Fundamentals and Applications, Wiley VCH, (2003).

[2] P. R. Sreenivasan and S. K. Ray: Mechanical Testing at High Strain Rates. Encyclopaedia of Materials: Science and Technology (2008), p. 5269

[3] H. Kolsky: Proc. Phys. Soc. B62 (1949), p. 676

[4] H. Zhao, G. Gary: Int. J. Solids Structures, 33 (23) (1996), p. 3363

[5] W. Chen, B. Song, D. Frew, M. Forrestal: Exp. Mech., 43 (1) (2002), p. 20

[6] L. M. Yang, V. P. W. Shim: Int. J. Imp. Eng. 31 (2) (2005), p. 129

[7] E. D. H. Davies, S. C. Hunter: J. Mech. Phys. Solids 11 (1963), p. 155

[8] L. D. Bertholf, J. Karnes: J.Mech. Phys. Solids 23(1975), p. 1

[9] J. F. Bell: J. Mech. Phys. Solids 14 (1966), p. 309

[10] T. Vuoristo and V.-T. Kuokkala: Mech. Mater. 34 (8) (2002), p. 493

[11] M. Hokka: Mechanical testing of materials with the Hopkinson Split Bar technique in proceedings of the SMP IX Conference, Lappeenranta, Finland (2006).

[12] Z. Li and J. Lambros: Compos. Sci. Technol. 59 (7) (1999), p. 1097

[13] M. Hokka: Effects of Strain Rate and Temperature on the Mechanical Behavior of Advanced High Strength Steels. Ph.D. thesis, Department of Materials Science, Tampere University of Technology (2008).

[14] MSC. Marc User's Guide, Version 2008r1, MSC Software Corporation, Los Angeles (2008).

[15] M. Demiral, A. Roy and V.V. Silberschmidt: Effects of loading conditions on deformation process in indentation, Comp., Mater. & Cont. (2010) (submitted).

[16] M.A. Meyers, Y.J. Chen, F.D.S. Marouis and D.S. Kim: Metall. Mater. Trans. A 26 (1995), p. 2493

[17] Y. Wang, Y.X. Zhou and Y.M. Xia: Mater. Sci. Eng. A 372 (2004), p. 186